

Cite this: *Chem. Commun.*, 2012, **48**, 9708–9710

www.rsc.org/chemcomm

High performance metal–organic-framework coatings obtained *via* thermal gradient synthesis†

Felix Jeremias,^{ab} Stefan K. Henninger^{*a} and Christoph Janiak^{*b}

Received 4th July 2012, Accepted 9th August 2012

DOI: 10.1039/c2cc34782b

For many possible applications of metal–organic frameworks, a coating onto a metallic support capable of both superior heat and mass transfer is required. A heated substrate in contact with a chilled solution of metal salt and linker reproducibly yields polycrystalline, highly stable, thermally conductive MOF coatings at a growth rate of $50 \mu\text{m h}^{-1}$, illustrated by the formation of $\text{Cu}_3(\text{btc})_2$ as an example.

The unmatched porosity of metal–organic frameworks¹ combined with a very high chemical variability² can be exploited especially well if these materials are produced in the shape of a film or coating.³ This has been proven for many potential applications like sensing, heterogeneous catalysis or the separation of gases and liquids. One of the most studied MOFs is copper trimesate (“HKUST-1”), because of easy formation,⁴ high porosity and known properties associated with this compound.⁵

The general synthetic approach towards MOF films is to induce preferential crystallite growth at the surface which is to be coated, compared to the surrounding solution. This can be achieved in a first step by various seeding techniques: MOF films, often with a specific orientation, have been obtained on substrates furnished with MOF nanocrystals or linker-containing entities like native hydroxyl groups or self-assembled monolayers (SAMs). In a second step this pre-conditioned surface is subjected to solvothermal synthesis conditions or layer-by-layer growth.⁶ A different method, which yields polycrystalline films, consists of delivering the required metal salt only to the surface to be coated. This has been achieved by (electro) chemical oxidation of a metal substrate, thus generating the required cations.⁷ Even air oxygen has been employed as a metal oxidant.⁸ Preferred MOF nucleation has also been observed on substrates coated with conductive layers which were subjected to microwave irradiation under solvothermal conditions.⁹

Most of the methods presented so far yield well-defined, uniform thin films, but require elaborate substrate preparation, and/or allow for slow growth rates only. This results in long reaction times, limited coated areas and layer thicknesses, thus, narrowing the possible range of applications. Other, inherent disadvantages consist of insufficient layer adhesion or product losses due to unwanted bulk crystallization from solution.^{6,7,10}

Here, we present a versatile, easy, fast, efficient and reproducible single-step route towards dense MOF coatings of virtually unlimited thicknesses with strong mechanical adhesion, accessible on various substrates. This was realized *via* a novel thermal gradient approach, as depicted in Fig. 1: the substrate which is to be coated is immersed into a solution of both the metal salt and the linker molecule, similar to the one used for solvothermal bulk synthesis of the desired MOF. The solution is now actively chilled, while the substrate surface is heated to the temperature which is usually applied during solvothermal bulk synthesis. As a result, the temperature which is necessary for MOF formation exists only at the boundary layer between the solution and the surface which is to be coated. This allows for high deposition rates with negligible losses (*i.e.* bulk crystallization in the vessel) and excellent properties of the obtained layer, such as very high crystallinity and mechanical stability. No special pre-treatment of the substrate is necessary, except for sanding and tempering. Purification and activation of the obtained layer are achieved by repeated soaking in a suitable solvent, followed by drying.

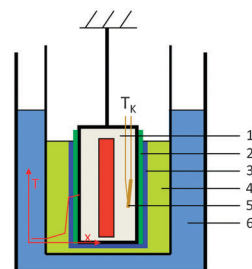


Fig. 1 Schematic cross-section of the experimental setup. The heater core (1) equipped with a surface thermocouple (5) is covered with the metal sheets to be coated (2) and immersed into a stirred $\text{Cu}(\text{NO}_3)_2\text{-H}_3\text{btc-DMF}$ solution (4). This assembly is surrounded by the cooling bath (6). HKUST-1 is deposited as a layer (3) on the metal sheet (2) due to the thermal gradient (red inset).

^a Department for Thermally Active Materials and Solar Cooling, Fraunhofer Institute for Solar Energy Systems (ISE), Heidenhofstr. 2, 79110 Freiburg, Germany. E-mail: stefan.henninger@ise.fraunhofer.de

^b Institut für Anorganische Chemie und Strukturchemie, Universität Düsseldorf, 40204 Düsseldorf, Germany. E-mail: janiak@uni-duesseldorf.de

† Electronic supplementary information (ESI) available: Detailed experimental setup and procedure, scanning electron micrographs, nitrogen sorption isotherm, XPS spectra, H_2O vapour cycling results, heat capacity measurements, details of all analytics. See DOI: 10.1039/c2cc34782b

Using the illustrated method, blue crystalline coatings of 100 μm thickness were produced repeatedly of consistent quality from $\text{Cu}(\text{NO}_3)_2$ -trimesic acid solution within 120 min onto a 5×5 cm Cu-support. The Cu metal size of 25 cm^2 can be enlarged. Copper sheets had been sanded and tempered at 120 $^\circ\text{C}$ for 12 h before. The colour of the coating changes reversibly from dark blue to turquoise when transferred from a dry atmosphere to ambient air. This behaviour is well known for HKUST-1.⁵

As can be seen from optical and SEM images (Fig. 2), the obtained coating consists of isotropic, highly intergrown crystallites of less than 10 μm size, but with a large size distribution. The presence of HKUST-1 as the major crystalline phase is confirmed by PXRD measurements (Fig. 3).

Nitrogen sorption experiments yielded a pore volume of $V_P = 0.58 \text{ cm}^3 \text{ g}^{-1}$ and a BET surface of $S_{\text{BET}} = 1160 \text{ m}^2 \text{ g}^{-1}$ for the crystalline top layer separated from the Cu surface (Fig. S5 in ESI[†]), which is considerably more than the value reported by Chui *et al.*,⁵ and approaches the value measured for bulk HKUST-1 synthesized in DMF ($V_P = 0.75 \text{ cm}^3 \text{ g}^{-1}$, $S_{\text{BET}} = 1507 \text{ m}^2 \text{ g}^{-1}$).¹¹ The deviation is due to the presence of unreacted trimesic acid, as can be seen from IR measurements (Fig. 4). The HKUST-1 coatings could be reproduced with a variance of their measured physical properties within 3% from 6 preparations on $5 \text{ cm} \times 5 \text{ cm}$ copper sheets.

In previous work, a “twin copper source” mechanism has been suggested for the growth of HKUST-1 on an oxidized copper mesh from a H_2O -ethanol solvothermal solution.¹² This means that the required Cu^{2+} ions are delivered not only from solution, but also from the copper oxide layer formed on top of the surface. In the present work, however, DMF was employed as a solvent, which is known to act as a reducing agent at elevated temperatures if H_2O is present.¹³ Hence, the first effect which could be observed at the beginning of the experiment was a rapid disappearance of the multi-coloured oxide layer that had been generated upon tempering. Successful HKUST-1 layer formation by this thermal gradient approach could be observed not only on copper, but also on aluminium and stainless steel sheets. Hence, it can be deduced that the substrate itself plays a minor role as a metal source under the applied conditions. The internal constitution of the obtained layer could be clarified by examination of a polished section with SEM/EDX (Fig. 4e and f). These measurements reveal that the obtained coating consists of two layers, a carbon-rich, thin bottom layer, and a more copper- and oxygen-rich, thick layer on top.

While the thicker top layer consists of HKUST-1 (proven by PXRD measurements, see Fig. 3), the chemical nature of the

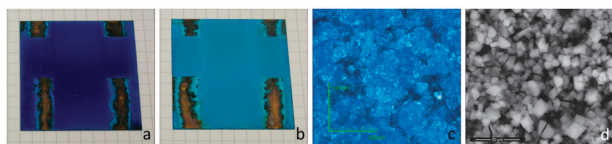


Fig. 2 Optical images of the obtained coated sheets after storing over CaCl_2 (a) and under ambient conditions (b). 1 square = $5 \times 5 \text{ mm}^2$. Optical microscope image (c) and SEM image (d). Note: bare copper areas in (a) and (b) are caused by mounting clamps (see Fig. S1a in ESI[†]). Cracks visible in (d) are not native to the layer, but due to electron bombardment.

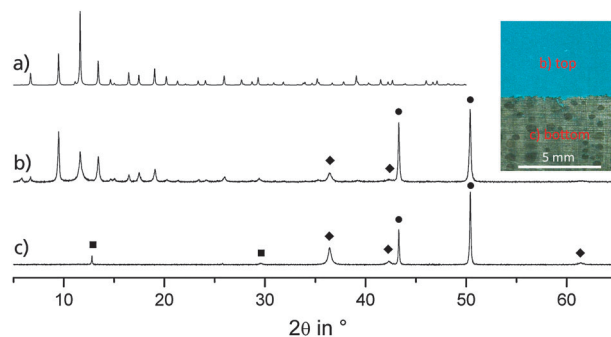


Fig. 3 Powder diffractograms for HKUST-1 (simulation, a), the synthesized coating (b) and the bottom layer (c). Assignments in (c): ■ = rouaite, $\text{Cu}_2(\text{NO}_3)(\text{OH})_3$, ◆ = Cu_2O , ● = Cu. The photograph is an on-top view onto the coating after removing the top layer in the lower part of the photograph so that the bottom layer can be seen.

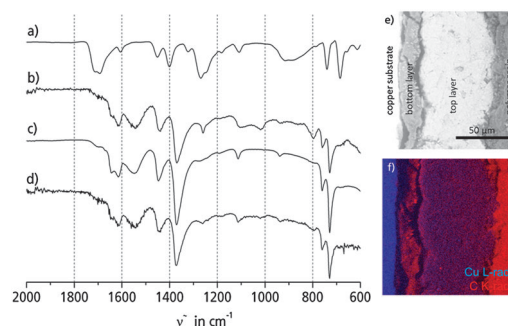


Fig. 4 FT-IR spectra (ATR) of the trimesic acid H3btc (a), thin separated bottom layer (b), the separated top layer (c), and the whole coating after purification with DMF and ethanol (see ESI[†] for details) (d). (e) SEM image, (f) EDX element mapping of a polished section of the coated Cu sheet, embedded in polymer resin. Cracks are due to electron bombardment. See Fig. S3 (ESI[†]) for separate element maps.

bottom layer is more complicated. High carbon content and traces of nitrogen were found by SEM/EDX, and XPS measurements (see Fig. S4 in ESI[†]). PXRD analysis of the bottom layer revealed the presence of crystalline $\text{Cu}_2(\text{NO}_3)(\text{OH})_3$ (rouaite) and Cu_2O . No PXRD reflections, however, could be assigned to the organic phase which apparently was amorphous.

Despite differences in elemental composition and crystallinity between the top and bottom layer from elemental analysis and PXRD, the IR spectrum of the bottom layer is very similar to that of the HKUST-1 top layer with additional bands in the fingerprint region at 1258, 1015 and 800 cm^{-1} (see Fig. 4). As the bottom layer was soluble neither in DMF, nor in EtOH or aqueous conc. NH_3 , a mostly organic, polymeric structure can be anticipated. This seems to be even more likely, as $\text{Cu}(\text{II})$, $\text{Cu}(\text{I})$ and $\text{Cu}(0)$ species are present in the reaction system, which are known to catalyse all kinds of coupling reactions even of non-halogenated arenes, especially if the system is exposed to air.¹⁴

The high carbon content in the bottom layer can be explained by a copper-catalysed decarboxylation of aromatic carboxylic acids. Such a decarboxylation reaction has already been observed and used for organic synthesis with reaction conditions very similar to those employed in the present work.¹⁵

The obtained coating is of remarkable mechanical stability. No cracks, flaking or wear-off of any kind could be observed when handling samples without special care, although macropore-like

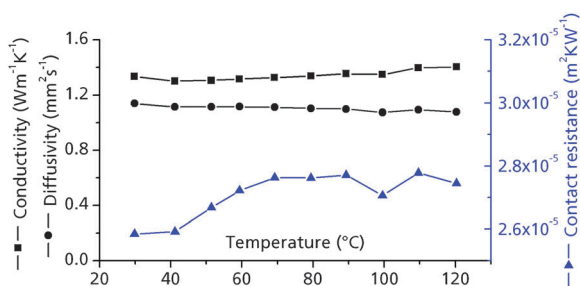


Fig. 5 Conductivity, diffusivity and contact resistance determined via laser flash analysis (see ESI† for details).

channels with a diameter of 30 to 50 μm could be observed between the crystals (see Fig. 2c and Fig. S8 in ESI†).

Even after 500 ad-/desorption cycles with H_2O vapour, which led to complete loss of the HKUST-1 structure as expected,¹⁶ mechanical adhesion remained unchanged (exact cycling conditions are given in the ESI†). Heat conduction properties of the activated coating from 30 to 120 $^\circ\text{C}$ have been determined by laser flash analysis (Fig. 5). A 2-layer Cowan model was used, with layer 1 as the Cu substrate, and layer 2 as the coating, averaging bottom and top layers. For the coating, a density of 1.22 g cm^{-3} has been anticipated,⁵ while the c_p curve was obtained from a calorimetric measurement of commercial copper trimesate (Basolite™ C300). Exact parameters are given in the ESI.†

The thermal conductivity of the coating, which lies in the range of 1.2 to $1.4\text{ W m}^{-1}\text{ K}^{-1}$ (Fig. 5), is very high compared to related materials with similar porosities, like activated carbon beds (0.15 to $0.5\text{ W m}^{-1}\text{ K}^{-1}$),¹⁷ or silica gel packings ($0.2\text{ W m}^{-1}\text{ K}^{-1}$).¹⁸ This can be explained by the fact that the crystallites are highly intergrown and, hence, heat transfer is facilitated compared to a loose packing of particles or beads. The contact resistance between the copper substrate and the coating ranges from $2.6 \times 10^{-5}\text{ m}^2\text{ K W}^{-1}$ to $2.8 \times 10^{-5}\text{ m}^2\text{ K W}^{-1}$ in the examined temperature range (25–150 $^\circ\text{C}$, Fig. 5), which is an excellent figure for a MOF/metal interface. For comparison, a very good value for the contact resistance between two plain copper sheets, obtainable via soldering, is about $5 \times 10^{-6}\text{ m}^2\text{ K W}^{-1}$.¹⁹

In summary, we have introduced a novel and widely applicable method to deposit polycrystalline layers of metal–organic frameworks at unprecedented growth rates. Our results show that the thermal gradient approach yields highly porous and mechanically stable coatings of HKUST-1, which also exhibits high thermal coupling to the substrate. These properties are especially beneficial for coating heat exchangers in sorption heat pumps,²⁰ for catalysis or gas storage applications.

We thank the Federal German Ministry of Economics (BMWi) for grant 0327851A/B.

Notes and references

- G. Férey, *Chem. Soc. Rev.*, 2008, **37**, 191–214; S. Kitagawa, R. Kitaura and S.-I. Noro, *Angew. Chem., Int. Ed.*, 2004, **43**, 2334–2375; H. Wu, Q. Gong, D. H. Olson and J. Li, *Chem. Rev.*, 2012, **112**, 836–868; C. Janiak and J. K. Vieth, *New J. Chem.*, 2010, **34**, 2366–2388; P. Horcajada, R. Gref, T. Baati, P. K. Allan, G. Maurin, P. Couvreur, G. Férey, R. E. Morris and C. Serre,

- Chem. Rev.*, 2012, **112**, 1232–1268; N. Stock and S. Biswas, *Chem. Rev.*, 2012, **112**, 933–969; J.-Y. Lee, O. K. Farha, J. Roberts, K. Scheidt, S. T. Nguyen and J. T. Hupp, *Chem. Soc. Rev.*, 2009, **38**, 1450–1459.
- K. Sumida, D. L. Rogov, J. A. Mason, T. M. McDonald, E. D. Bloch, Z. R. Herm, T.-Y. Bae and J. R. Long, *Chem. Rev.*, 2012, **112**, 724–781; S. M. Cohen, *Chem. Sci.*, 2010, **1**, 32–36; M. O’Keeffe, *Chem. Soc. Rev.*, 2009, **38**, 1215–1217; R. J. Kuppler, D. J. Timmons, Q.-R. Fang, J.-R. Li, T. A. Makal, M. D. Young, D. Yuan, D. Zhao, W. Zhuang and H.-C. Zhou, *Coord. Chem. Rev.*, 2009, **253**, 3042–3066; S. Kitagawa and R. Matsuda, *Coord. Chem. Rev.*, 2007, **251**, 2490–2509; C. Janiak, *Dalton Trans.*, 2003, 2781–2804; T. K. Maji and S. Kitagawa, *Pure Appl. Chem.*, 2007, **79**, 2155–2177; L. J. Murray, M. Dinca and J. R. Long, *Chem. Soc. Rev.*, 2009, **38**, 1294–1314.
- R. A. Fischer and A. Bétard, *Chem. Rev.*, 2012, **112**, 1055–1083; L. E. Kreno, K. Leong, O. K. Farha, M. Allendorf, R. P. Van Duyne and J. T. Hupp, *Chem. Rev.*, 2012, **112**, 1105–1125; O. Shekhhah, J. Liu, R. A. Fischer and C. Wöll, *Chem. Soc. Rev.*, 2011, **40**, 1081–1106; J. Gascon and F. Kapteijn, *Angew. Chem., Int. Ed.*, 2010, **49**, 1530–1532.
- Q. M. Wang, D. Shen, M. Bülow, M. L. Lau, S. Deng, F. R. Fitch, N. O. Lemcoff and J. Semancin, *Microporous Mesoporous Mater.*, 2002, **55**, 217–230; K. Schlichte, T. Kratzke and S. Kaskel, *Microporous Mesoporous Mater.*, 2004, **73**, 81–88.
- H. C. Jeong, B. Samanta, C. Y. Lee, O. K. Farha and J. T. Hupp, *J. Am. Chem. Soc.*, 2012, **134**, 51–54; R. Q. Snurr, A. O. Yazaydin, A. I. Benin, S. A. Faheem, P. Jakubczak, J. J. Low and R. R. Willis, *Chem. Mater.*, 2009, **21**, 1425–1430; S. S.-Y. Chui, S. M.-F. Lo, J. P. H. Charmant, A. G. Orpen and I. D. Williams, *Science*, 1999, **283**, 1148–1150.
- J. Gascon, S. Aguado and F. Kapteijn, *Microporous Mesoporous Mater.*, 2008, **113**, 132–138.
- U. Mueller, M. Schubert, F. Teich, H. Puetter, K. Schierle-Arndt and J. Pastré, *J. Mater. Chem.*, 2006, **16**, 626–636.
- S. Kayaert, S. Bajpe, K. Masschaele, E. Breynaert, C. E. A. Kirschhock and J. A. Martens, *Thin Solid Films*, 2011, **519**, 5437–5440.
- Y. Yoo and H.-K. Jeong, *Chem. Commun.*, 2008, 2441–2443.
- V. V. Guerrero, Y. Yoo, M. C. McCarthy and H.-K. Jeong, *J. Mater. Chem.*, 2010, **20**, 3938–3943; Y.-S. Li, F.-Y. Liang, H. Bux, A. Feldhoff, W.-S. Yang and J. Caro, *Angew. Chem., Int. Ed.*, 2010, **49**, 548–551; Y.-S. Li, H. Bux, A. Feldhoff, G.-L. Li, W.-S. Yang and J. Caro, *Adv. Mater.*, 2010, **22**, 3322–3326; D. Zacher, O. Shekhhah, C. Wöll and R. A. Fischer, *Chem. Soc. Rev.*, 2009, **38**, 1418–1429; R. Ameloot, L. Stappers, J. Fransaer, L. Alaerts, B. F. Sels and D. E. De Vos, *Chem. Mater.*, 2009, **21**, 2580–2582; R. Ameloot, L. Pandey, M. Van der Auweraer, L. Alaerts, B.-F. Sels and D. E. De Vos, *Chem. Commun.*, 2010, **46**, 3735–3737.
- J. L. C. Rowsell and O. M. Yaghi, *J. Am. Chem. Soc.*, 2006, **128**, 1304–1315.
- H. Guo, G. Zhu, I.-J. Hewitt and S. Qiu, *J. Am. Chem. Soc.*, 2009, **131**, 1646–1647.
- P. K. Khanna, P. More, Y. Patil, J. Jawalkar, D. Kulkarni and A. Dhangar, *Synth. React. Inorg., Met.-Org., Nano-Met. Chem.*, 2009, **39**, 221–224.
- G. Evano, N. Blanchard and M. Toumi, *Chem. Rev.*, 2008, **108**, 3054–3131.
- L. J. GooBen, W. R. Thiel, N. Rodriguez, C. Linder and B. Melzer, *Adv. Synth. Catal.*, 2007, **349**, 2241–2246.
- P. Küsgens, M. Rose, I. Senkovska, H. Fröde, A. Henschel, S. Siegle and S. Kaskel, *Microporous Mesoporous Mater.*, 2009, **120**, 325–330; M. Schlesinger, S. Schulze, M. Hietschold and M. Mehring, *Microporous Mesoporous Mater.*, 2010, **132**, 121–127.
- D. Menard, X. Py and N. Mazet, *Chem. Eng. Process.*, 2007, **46**, 565–572.
- J. Gurgel and R. Klüppel, *Chem. Eng. J.*, 1996, **61**, 133–138.
- C. Leong and D. Chung, *Carbon*, 2003, **41**, 2459–2469.
- F. Jeremias, A. Khutia, S. K. Henninger and C. Janiak, *J. Mater. Chem.*, 2012, **22**, 10148–10151; S. K. Henninger, F. Jeremias, H. Kummer and C. Janiak, *Eur. J. Inorg. Chem.*, 2012, 2625–2634; J. Ehrenmann, S. K. Henninger and C. Janiak, *Eur. J. Inorg. Chem.*, 2011, 471–474.